

Velocity autocorrelation function of a dispersion of heavy particles in a turbulent flow: on the effect of interparticle collisions

R. Avila^{a,c} and M.A. Rodríguez-Meza^{b,c}

^a Facultad de Ingeniería, Universidad Nacional Autónoma de México,
Apartado Postal 1405, México D.F., México,

^b Instituto de Física, Universidad Autónoma de Puebla,
Apartado Postal J-48, 72570 Puebla, México,

^c Depto. de Física, Instituto Nacional de Investigaciones Nucleares,
Apartado Postal 18-1027, 11801 México D.F., México

Recibido el 6 de marzo de 2003; aceptado el 27 de agosto de 2003

The effect of particle-to-particle interactions on the dispersion and on the velocity auto-correlation function of heavy particles in a turbulent flow, is presented. The inter-particle collision process is based on a direct numerical simulation approach, which requires that all the particles be simultaneously tracked through the flow field. In the first part of the paper, the turbulent characteristics of the velocity of non-colliding heavy particles which disperse in a vertical, nearly isotropic, grid generated decaying turbulence air flow, are presented. In the second part of this investigation, the solid particles are allowed to collide. The numerical predictions confirm the fact that the inter-particle collisions promote a decrease of the lateral particle dispersion, the particle velocity autocorrelation function and the mean lateral velocity of the particles.

Keywords: Particle dispersion; velocity autocorrelation function; turbulent flows

Se presentan los efectos de las interacciones entre partículas sobre la dispersión y sobre la función de auto-correlación de velocidades de partículas pesadas en un flujo turbulento. Los procesos de colisión entre partículas está basado en una simulación numérica directa, que requiere que todas las partículas sean simultáneamente seguidas a través del campo de flujo. En la primera parte del artículo se presentan las características turbulentas de las velocidades de partículas pesadas y sin colisión que se dispersan en un flujo de aire turbulento decayente vertical, casi isótropo y generado por una malla. En la segunda parte de esta investigación se les permite a las partículas sólidas colisionar. Las predicciones numéricas confirman el hecho de que las colisiones entre partículas promueve una disminución de la dispersión lateral de las partículas, de la función de autocorrelación de velocidad y de la velocidad media lateral de las partículas.

Descriptores: Dispersión de partículas; función de autocorrelación de velocidades; flujos turbulentos

PACS: 47.27.Gs; 47.55.Kf; 45.50.Tn

1. Introduction

The prediction of the dispersion and concentration of heavy particles in a turbulent flow, is a very important task in some industrial processes and natural phenomena. Examples are the atmospheric spread of radioactive or chemical pollutants, and the atmospheric transport of rain, sand, dust and ash.

When a particle with a diameter much smaller than the Kolmogorov scale is transported in a turbulent flow, the interaction between it and its surrounding fluid, may be in “one way”. However as the particle mass loading ratio begins to increase, the suspended heavy particles may also modify the turbulent energy of the carrier fluid (“two-way coupling”). When the particle number density increases further more, the particles begin to dynamically interact between them. In this situation, the inter-particle interaction may partially governs the dispersion and turbulent properties of the particulate phase. This is the so called “four-way coupling”, which has been the subject of much effort in the recent years [1–7].

Tanaka and Tsuji [1] used a direct approach (very similar to the one presented in this paper) to determine the effect of inter-particle collisions on the velocity and concentration of particles, in a fully developed vertical gas-particle pipe flow. Tanaka and Tsuji [1] found that inter-particle col-

lisions, have a large effect on the dispersion of particles even at small solids volume fraction. They also found that as the solid loading increases, the particle velocity profiles become increasingly isotropic.

The solids volume fraction, defined as $\alpha = nV_p/V_T$, where n is the total number of particles in the volume V_T , and V_p is the volume of an individual particle, is a useful quantity to determine the importance of the inter-particle collisions on the properties of the dispersed particles. For example, Tanaka and Tsuji [1] used in their predictions values of α in the interval $1.0 \times 10^{-4} \leq \alpha \leq 1.0 \times 10^{-2}$. In our simulations we used $\alpha = 0.0089$.

Lavieville *et al.* [6] have reported that if standard Lagrangian approaches are used to predict the dispersion of non-settling, colliding, elastic particles in a turbulent flow, it results (as the collision frequency increases) in:

- (i) an appreciable decrease of the effective particle dispersion coefficient,
- (ii) a decrease of the particle kinetic energy and
- (iii) a decrease of the fluid-particle velocity covariance.

They have mentioned that these effects appear, due to the destruction of the fluid-particle velocity correlation that takes place during the collision process.

More recently Sommerfeld [7] introduced a Lagrangian one way model, that takes into account the correlation of the velocities of colliding particles in a homogeneous isotropic turbulence. Sommerfeld assumed that the velocities of colliding particles are correlated, since they are within the same turbulent eddy during the collision process.

In this paper the effect of particle-to-particle interactions on the dispersion and the velocity autocorrelation function of spherical heavy particles that are transported in a vertical decaying turbulence is presented. The calculation of the interparticle collision process is based on a “one way”, standard, direct numerical simulation approach, which requires that all the particles be simultaneously tracked through the flow field [1]. In the momentum equations of the particles, the body force and the drag force are included. The interparticle collision detection model is based on a hierarchical Tree-algorithm [8], which efficiently performs the search of the nearest neighbors of each particle (the “pilot” particle). Once the neighbors of the “pilot” particle are identified, a number of transcendental equations are solved to predict the possible collision time between the pair of particles. The fully elastic post-collision position and the velocity components of the colliding particles, are obtained by solving the impact equations under the assumptions of an instantaneous binary collision and a very small contact surface [9]. The successive velocity fluctuations of the fluid elements seen by a heavy particle are generated (by using a Monte Carlo procedure) as Gaussian random numbers with standard deviation given by the local turbulent characteristics of the flow field [10, 11].

The model is used to predict the dispersion of heavy particles, which are released, as an instantaneous “puff” into a vertical, grid generated decaying turbulence air flow. In the first part of the paper, the trajectory of each particle is calculated by assuming that the particles in the cluster do not collide. The non-interacting particle results (obtained in a vertical rectangular parallelepiped domain with lateral periodic boundaries) compare successfully with the experimental data published in the literature [12]. In the second part of the paper the particles in the instantaneous “puff” are allowed to collide. In order to promote a great number of inter-particle collisions and to quantify the real influence of this phenomenon on the particle dispersion and on the particle velocity autocorrelation function, the computational domain was also defined as a vertical rectangular parallelepiped with lateral periodic boundaries. The numerical predictions confirm the fact that the inter-particle collisions promote a decrease of the following:

- (i) the lateral particle dispersion,
- (ii) the particle velocity autocorrelation function and
- (iii) the mean lateral velocity of the particles.

2. Lagrangian Approach

In the numerical predictions, it is assumed that the drag and the gravity are the only forces acting on the spherical parti-

cles. Hence, in order to know the trajectory of each individual particle, we solve the following set of Lagrangian equations:

$$\frac{du_{ip}}{dt} = \frac{u_i - u_{ip}}{\tau_p} - \delta_{i2}g \left(1 - \frac{\rho}{\rho_p}\right), \quad (1)$$

where u_i are the instantaneous velocities of the fluid and u_{ip} are the instantaneous velocities of the particles ($i=1,2,3$). The instantaneous velocity of the fluid is defined as $u_i = \bar{U}_i + u'_i$. The dynamic characteristic time of the particle is defined as $\tau_p = m_p / (3\pi\mu f d_p)$, where μ and ρ are the dynamic viscosity and density of the fluid respectively, g is the gravity acceleration, and ρ_p , m_p and d_p , are the density, mass and diameter of the particle respectively. The non-linear drag coefficient is given by $f = 1 + 0.15\text{Re}_p^{0.687}$, where the particle Reynolds number is $\text{Re}_p = \rho d_p U_{rel} / \mu$, and U_{rel} is the relative velocity between the particle and its surrounding eddy [10].

The fluid velocity fluctuations (u'_i) seen by the particles along their trajectory, are generated as Gaussian random numbers with standard deviation given by the local variances $\overline{u'^2_i}$ [11]. A standard Monte-Carlo process, without memory between two successive fluid velocity fluctuations seen by a particle, has been used. The interacting time (particle-eddy), also known as eddy-life time, and the length scale of the eddy surrounding each particle, are determined as functions of the local turbulent characteristics of the flow, *i.e.*, $T_I = 0.3\kappa/\epsilon$ and $L_I = (2\kappa/3)^{1/2} T_I$, where κ and ϵ are the turbulent kinetic energy and its dissipation rate respectively [10].

For small time intervals t (less than the eddy-life time and less than the collision time with another particle), the solution of the Eqs. (1) is as follows:

$$u_{ip} = u_i - (u_i - u_{ip0}) \exp(-t/\tau_p) - \delta_{i2}g \left(1 - \frac{\rho}{\rho_p}\right) [1 - \exp(-t/\tau_p)] \tau_p, \quad (2)$$

where u_{ip0} are the initial velocities of the particles (at $t = 0$).

3. Collision Detection Algorithm

The collision detection algorithm is based on the solution of a transcendental equation which is a function of the relative position between two particles (a “pilot” particle and its neighbor). If one zero (collision time) of the transcendental equation is found, it means that the pair of particles will collide after this time. A hierarchical Tree algorithm (Tree-structured data) is used to efficiently search the particles that are located in the near neighborhood of the “pilot” particle [8]. In the detection collision algorithm it is assumed that after a small time increment t , the “pilot” particle is at the new position $\mathbf{c} = \mathbf{x}_o + \mathbf{u}_p t$, where \mathbf{x}_o is the particle initial position vector and \mathbf{u}_p is the particle velocity vector. It is also assumed that after the same small time increment t , the neighbor particle is at the new position $\bar{\mathbf{c}} = \bar{\mathbf{x}}_o + \bar{\mathbf{u}}_p t$, where the overbar refers to

the neighbor particle. In the numerical procedure a collision occurs when $\mathbf{c} + \mathbf{d} = \bar{\mathbf{c}}$, where the magnitude of the vector \mathbf{d} is the sum of the radii of the particles $|\mathbf{d}| = r_p + \bar{r}_p$. Using

$$\begin{aligned} & \left[t(\bar{u} - (\bar{u} - \bar{u}_{po}) \exp(-t/\bar{\tau}_p) - u + (u - u_{po}) \exp(-t/\tau_p)) + (\bar{x}_o - x_o) \right]^2 \\ & + \left[t\left(\bar{v} - (\bar{v} - \bar{v}_{po}) \exp(-t/\bar{\tau}_p) - g\left(1 - \frac{\rho}{\rho_p}\right) \left[1 - \exp(-t/\bar{\tau}_p)\right] \bar{\tau}_p \right. \right. \\ & \quad \left. \left. - v + (v - v_{po}) \exp(-t/\tau_p) + g\left(1 - \frac{\rho}{\rho_p}\right) \left[1 - \exp(-t/\tau_p)\right] \tau_p \right) + (\bar{y}_o - y_o) \right]^2 \\ & + \left[t(\bar{w} - (\bar{w} - \bar{w}_{po}) \exp(-t/\bar{\tau}_p) - w + (w - w_{po}) \exp(-t/\tau_p)) + (\bar{z}_o - z_o) \right]^2 = (r_p + \bar{r}_p)^2. \quad (3) \end{aligned}$$

Here, $x_o, y_o,$ and z_o are the components of \mathbf{x}_o ; $u_{po}, v_{po},$ and w_{po} are the components of \mathbf{u}_p ; and $u, v,$ and w are the components of \mathbf{u} the velocity of the neighbor fluid. Similar notation is used for the neighbor particle. The solution of the Eq. (3) provides the collision time between the ‘‘pilot’’ particle and the neighbor particle.

4. Collision Model

Once the minimum collision time has been found (between all the collision times detected), the new position of all the particles in the flow field is calculated by using, as time increment, the minimum collision time. After this time, two particles are in contact, so the collision model is applied. In the collision model it is assumed the following:

- (i) the impact has a short duration time,
- (ii) sudden changes occur in the velocities of the particles,
- (iii) two ideal elastic, rough spherical particles collide (binary collision assumption) with velocities \mathbf{v}_1 and \mathbf{v}_2 (the subindex 1 is for the ‘‘pilot’’ particle and the subindex 2 is for the neighbor particle) and
- (iv) the kinetic energy and the linear and angular momentum are conserved.

After the collision, the velocities of the particles are \mathbf{v}'_1 and \mathbf{v}'_2 . The state of the particles after the collision is obtained by solving the following equations of impulsive motion [1, 9]

$$\begin{aligned} m_1 \mathbf{v}'_1 &= m_1 \mathbf{v}_1 + \delta \mathbf{p}, \\ m_2 \mathbf{v}'_2 &= m_2 \mathbf{v}_2 - \delta \mathbf{p}, \\ \bar{\omega}'_1 &= \bar{\omega}_1 + \frac{r_1}{r_1 + r_2} \mathbf{r}_{12} \times \delta \mathbf{p} / I_1, \\ \bar{\omega}'_2 &= \bar{\omega}_2 + \frac{r_2}{r_1 + r_2} \mathbf{r}_{12} \times \delta \mathbf{p} / I_2, \end{aligned} \quad (4)$$

the trajectory equations, the collision condition equation and the velocity Eqs. (2), the following transcendental equation is formulated:

where m_1, m_2, r_1, r_2, I_1 and I_2 are the masses, radii and moments of inertia of the particles 1 and 2. The vector \mathbf{r}_{12} corresponds to the vector \mathbf{d} of the previous section, hence when the particles are in contact, this vector joins the centre of the particle 1 with the centre of the particle 2. The vector $\delta \mathbf{p}$ is the collision impulsive force. This force has two components

- (i) the normal component (parallel to the vector \mathbf{r}_{12}) and
- (ii) the tangential component (perpendicular to the vector \mathbf{r}_{12}).

For ideal rough spheres, the tangential component is given by

$$\delta p^\perp = \left(\frac{4}{7}\right) \frac{|\mathbf{V}_{12}^{imp\perp}|}{1/m_1 + 1/m_2}. \quad (5)$$

In the Eq. (5) it has been assumed that the magnitude of the slip velocity vector after the collision $|\mathbf{V}_{12}^{imp\perp}'|$ is equal to the negative of the magnitude of the slip velocity vector before the collision (rough spheres), *i.e.*,

$$|\mathbf{V}_{12}^{imp\perp}'| = -|\mathbf{V}_{12}^{imp\perp}|. \quad (6)$$

5. Results

The Lagrangian approach is used to predict the dispersion of heavy particles (without and with collisions) in a vertical, nearly isotropic, grid generated, homogeneous, decaying turbulent air flow [12]. In the experiment of Snyder and Lumley (1971), particles of different size and material (ranged from light to heavy particles, see Table I) were injected at the position $y/M=20$, where y is the distance from the grid and $M=2.54$ cm is the grid spacing. The experimental air flow turbulence data are the following:

- (1) the mean vertical upward (streamwise direction) air velocity $\bar{V} = 6.55$ m/s,

- (2) the mean lateral and transverse velocities $\overline{U} = \overline{W} = 0$ m/s,
- (3) the energy decay in the streamwise direction $(\overline{V})^2 / v'^2$,
- (4) the energy decay in the lateral and transverse direction $(\overline{V})^2 / u'^2 = (\overline{V})^2 / w'^2$,
- (5) the turbulent kinetic energy κ and
- (6) the turbulent dissipation rate ϵ .

In order to predict the dispersion, the lateral velocity decay and the autocorrelation function of the particles, 12,800 heavy particles were instantaneously released (with an initial separation between them of one particle diameter) at the position $y/M=20$ ($y=0.508$ m). The particles are simultaneously tracked along the vertical streamwise direction from $y/M=20$ to $y/M=171$. In the numerical predictions, the air density and the kinematic viscosity are $\rho=1.205$ Kg/m³ and $\nu=14.93 \times 10^{-6}$ m²/s respectively. The density and the diameters of the solid particles are shown in Table I.

Figure 1 shows the lateral particle dispersion and the fluctuating lateral particle velocity decay for non-colliding particles. It may be observed that the lateral dispersion is in agreement with the experimental data. It is shown that the lateral fluctuating velocity of the heavier particles (copper and glass)

is well predicted after 400 ms. It means that at short distances from the grid, the energy of the heavier particles in the experiment was higher than in the simulations. It may be argued that in the experiment, the particles at the point of injection probably had an initial lateral movement. It is observed that for the lighter particles (hollow glass), the computations provide higher lateral fluctuating velocity. A reason of this behaviour probably is due to the Monte Carlo model used to generate the fluid velocity fluctuations of the fluid elements seen by the particles.

Figure 2 shows the numerical simulations of the lateral particle dispersion and the fluctuating lateral particle velocity for non-colliding and colliding particles. It is clearly observed that, due to the effect of the collisions, the dispersion of all the particles is reduced. It is also observed that (when the collisions are included) the lateral fluctuating velocity is

TABLE I. Diameter and density of the particles used in the experiment of Snyder and Lumley (1971)

	Hollow glass	Corn pollen	Glass	Copper
Diameter (μm)	46.5	87.0	87.0	46.5
Density (Kg/m ³)	260	1000	2500	8900

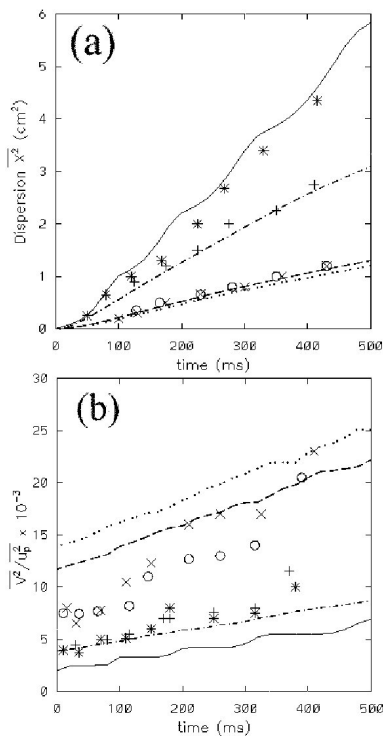


FIGURE 1. (a) Lateral particle dispersion $\overline{X^2}$. (b) Fluctuating lateral u_p^2 particle velocity. Both figures without collisions. Comparison between experimental data (symbols), and numerical predictions (lines). Copper: dotted line and (x), Glass: dashed line and (o), Corn pollen: dashed-dotted line and (+), Hollow glass: solid line and (*).

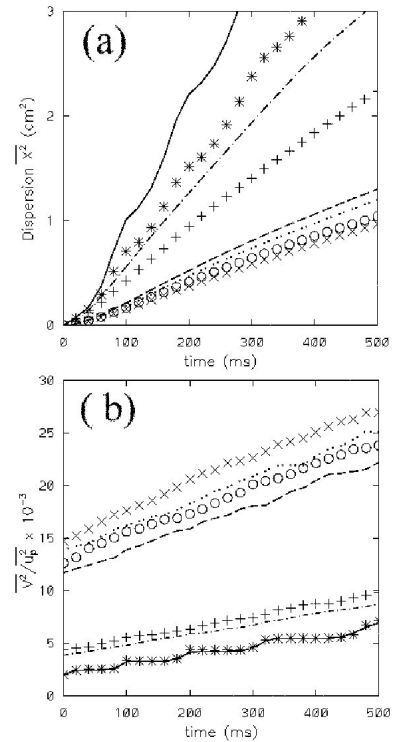


FIGURE 2. (a) Lateral particle dispersion $\overline{X^2}$. (b) Fluctuating lateral u_p^2 particle velocity. Both figures without and with collisions. Numerical predictions without collisions (lines), with collisions (symbols). Copper: dotted line and (x), Glass: dashed line and (o), Corn pollen: dashed-dotted line and (+), Hollow glass: solid line and (*).

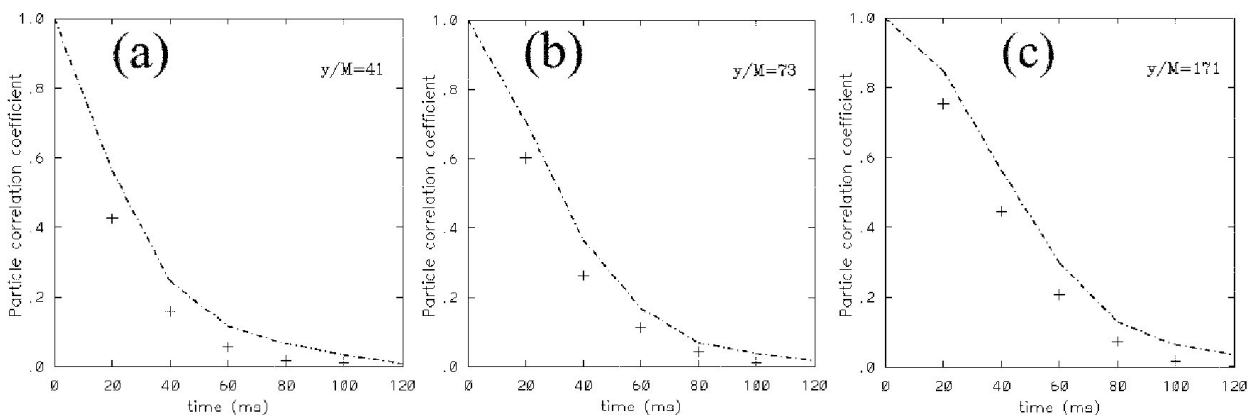


FIGURE 3. Particle velocity autocorrelation coefficient R_{11} (see Eq.(7)) at three positions along the longitudinal direction ($y/M=41, 73$ and 171). Corn pollen particles without collisions (dashed-dotted line) and with collisions (+). Total number of binary collisions 49,769.

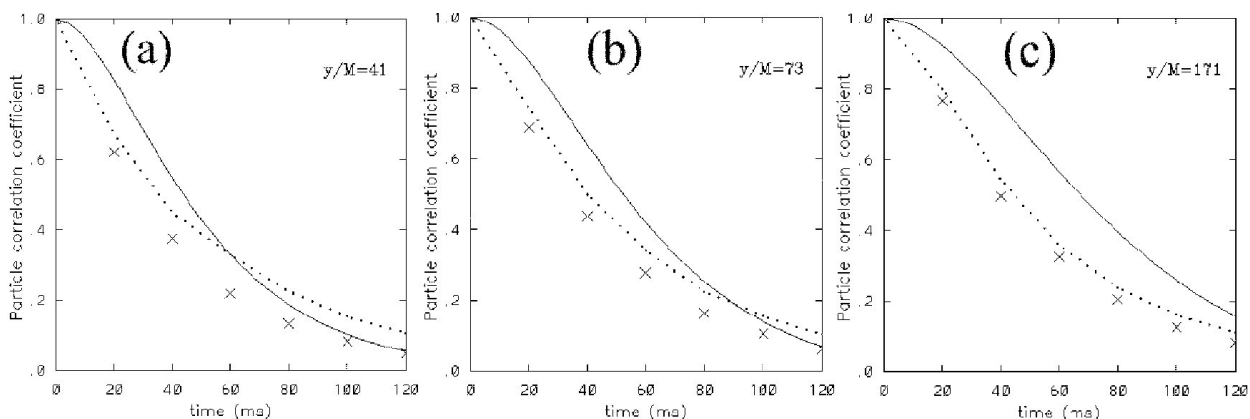


FIGURE 4. Particle velocity autocorrelation coefficient R_{11} (see Eq.(7)) at three positions along the longitudinal direction ($y/M=41, 73$ and 171). Copper particles, comparison between numerical predictions (without collisions dotted line, with collisions (x)) and the analytical solution without collisions (solid line) [13]. Total number of binary collisions 42,307.

remarkably reduced for the heavier particles (inertia effects). It is interesting to observe that for the hollow glass particles, the lateral velocities with and without collisions are almost the same, it means that after the collisions, the hollow glass particles immediately respond to the velocity fluctuations of the surrounding fluid, so the reduction of the lateral dispersion is mainly due to the restriction of the lateral movement imposed by the presence of the neighbours (collisions).

The lateral particle velocity autocorrelation coefficient R_{11} , for non-colliding and colliding particles has been calculated at three positions along the longitudinal direction $y/M=41, 73$ and 171 . The autocorrelation coefficient defined as

$$R_{11} = \frac{\overline{u_p(\Delta t) u_p(0)}}{u_p^2(0)} \quad (7)$$

is shown in Figs. 3 and 4 for corn pollen particles and copper particles respectively. Both figures show that the correlation functions are not self similar along the vertical streamwise direction. It is observed that as the turbulence kinetic energy decays (larger distance from the grid) the computations predict an increase in the characteristic correlation time. A comparison of both figures shows that as the dynamic charac-

teristic time of the particles is increased a higher correlation is obtained. It is interesting to observe that the effect of the collisions is to reduce the autocorrelation function. Figure 4 also shows the analytical results which were obtained by integrating the equations describing the local particle velocity correlations (without collisions). These equations were developed by Nir and Pismen [13] under the assumption that the characteristic turbulent fluid velocity is much lower than the deterministic particle velocity relative to the fluid owing to the gravity force. The analytical results for copper particles without collisions, were obtained by using a modified particle time constant $\gamma=22.22 \text{ s}^{-1}$. In order to calculate the three-dimensional spectrum $E(\kappa)$ that appears in the local particle velocity correlations equations [13], the following empirical constants, $a_1 = 270, a_2 = 1700$ and $a_3 = 10$ were used. It is observed in Fig. 4 that the analytical results also confirm the fact that the correlation functions are not self similar.

6. Conclusions

A direct numerical simulation model for the prediction of particle dispersion has been used to study the effect of inter-particle collisions on the dispersion, fluctuating velocity and correlation velocity of particles that are transported in a verti-

cal decaying turbulent flow. The results confirm the fact that when a standard Lagrangian approach is used to predict the dispersion of colliding, elastic, rough particles it results in an appreciable decrease of the effective particle dispersion coefficient, a decrease of the particle velocity fluctuations and a decrease in the characteristic correlation time. We should

conclude that the numerical model developed during this investigation, may be used to verify the analytical models (of non-colliding and colliding particles) aimed to obtain the Lagrangian particle velocity correlation tensor, the fluid velocity correlation tensor at the points lying on a particle trajectory and the relative fluid-particle velocity correlation tensor.

-
1. T. Tanaka and Y. Tsuji, "Numerical simulation of gas-solid two-phase flow in a vertical pipe: on the effect of inter-particle collision", In *Gas-Solid Flows*, Vol. 121. Eds. D. E. Stock *et al.* (ASME FED, 1991) p. 123.
 2. B. Oesterle and A. Petitjean, *Int. J. Multiphase Flow* **19** (1993) 199.
 3. A. Berlemont, Z. Chang, and G. Gouesbet, "Simulation of particle collisions in a two phase pipe flow by using multiple particles lagrangian tracking", In *Third International Conference on Multiphase Flow, ICMF'98*. (Lyon, France, June 8-12, 1998).
 4. M. Sommerfeld, "The importance of inter-particle collisions in horizontal gas-solid channel flows", In *Gas-Particle Flows*, Vol. 228. Eds. D. E. Stock *et al.* (ASME FED, 1995) p. 335.
 5. C. K. K. Lun and H. S. Liu, *Int. J. Multiphase Flow* **23** (1997) 575.
 6. J. Lavieville, O. Simonin, A. Berlemont, and Z. Chang, *Validation of inter-particle collision models based on large eddy simulation in gas-solid turbulent homogeneous shear flow*. In *Proc. of the ASME FED, FEDSM'97*. Eds. D. E. Stock *et al.* (ASME FED, 1997).
 7. M. Sommerfeld, "Inter-particle collisions in turbulent flows: A stochastic Lagrangian Model", In *Proc. of Turbulence and Shear Flow Phenomena* (Santa Barbara, CA, USA, 1999).
 8. S. Pfalzner and P. Gibbon, *Many-body tree methods in physics* (Cambridge University Press, 1997).
 9. S. Chapman and T. G. Cowling, *The Mathematical Theory of Nonuniform Gases* (Cambridge University, Cambridge, 1960).
 10. R. Avila, *Simulación Numérica de la Dispersión de una Nube de Partículas Sólidas Liberada a la Atmósfera*. Doctoral Thesis, División de Estudios de Posgrado Facultad de Ingeniería Universidad Nacional Autónoma de México (1997).
 11. G.K. Batchelor, *The Theory of Homogeneous Turbulence* (Cambridge University Press, London, 1970).
 12. W.H. Snyder and J.L. Lumley, *J. of Fluid Mech. Part I* **48** (1971) 41.
 13. A. Nir and L.M. Pismen, *J. Fluid Mech.* **94** (1979) 369.